PAPER

Acoustically penetrable sonic crystals based on fluid-like scatterers

IOP Publishing Journal of Physics D: Applied Physics

J. Phys. D: Appl. Phys. **48** (2015) 025501 (9pp) doi:10.1088/0022-3727/48/2/025501

Acoustically penetrable sonic crystals based on fluid-like scatterers

A Cebrecos[1], V Romero-García[2], R Picó[1], V J Sánchez-Morcillo[1], M Botey[3], R Herrero[3], Y C Cheng[3] and K Staliunas[3,4]

[1] Instituto de Investigación para la Gestión Integrada de zonas Costeras, Universitat Politècnica de València, Paranimf 1 46730 Grao de Gandia, Spain
[2] LUNAM Université, CNRS, LAUM UMR 6613, Av. O. Messiaen, 72085 Le Mans, France
[3] Departament de Física i Enginyeria Nuclear, Universitat Politècnica de Catalunya, Colom 11, 08222 Terrassa, Spain
[4] Institució Catalana de Recerca i Estudis Avançats (ICREA), 08010 Barcelona, Spain

E-mail: virogar1@gmail.com

Received 6 August 2014, revised 27 October 2014
Accepted for publication 13 November 2014
Published 12 December 2014

Abstract

We propose a periodic structure that behaves as a fluid–fluid composite for sound waves, where the building blocks are clusters of rigid scatterers. Such building-blocks are penetrable for acoustic waves, and their properties can be tuned by selecting the filling fraction. The equivalence with a fluid–fluid system of such a doubly periodic composite is tested analytical and experimentally. Because of the fluid-like character of the scatterers, sound structure interaction is negligible, and the propagation can be described by scalar models, analogous to those used in electromagnetics. As an example, the case of focusing of evanescent waves and the guided propagation of acoustic waves along an array of penetrable elements is discussed in detail. The proposed structure may be a real alternative to design a low contrast and acoustically penetrable medium where new properties as those shown in this work could be experimentally realized.

Keywords: phononic crystals, sonic crystals, periodic structures

(Some figures may appear in colour only in the online journal)

1. Introduction

The propagation of acoustic waves through an inhomogeneous medium made of N obstacles or scatterers embedded in a fluid is a broad topic with applications in different fields [1, 2]. Such obstacles can be considered either as penetrable [3] or not penetrable [4]. Also, their spatial distribution can be ordered [5], as in some artificial materials as e.g. photonic or sonic/phononic crystals, or disordered [6], as some complex media found in nature as bubbly fluids or fish schools. It is general a complex problem involving many variables, but on the other hand it offers many possibilities to engineer wave propagation or to extract information about the medium.

During the last years, attention has been mostly paid to periodic systems, presenting unique dispersion properties. Those are mainly photonic crystals [7] for electromagnetic waves, sonic and phononic crystals [8, 9] for acoustic and elastic waves respectively, as well as periodic media for more exotic waves (plasmons, Bose–Einstein condensates (BECs) etc) have been also considered.

The paralelism with electromagnetic waves is often used to predict new phenomena in acoustics, based on the analogy between the theoretical description of both systems, since both waves obey, in some limits, similar scalar wave equations. It has been the case, for example, with bandgaps, negative refraction, self-collimation, etc.

Photonic cystals can be built to present low or high index contrast, using dielectric or metallic elements respectively. The former represents the case of a penetrable system, where waves can propagate inside the scatterer and resonate within it, while the latter is a case of not penetrable system, where the wave propagates only in the host medium. Most of the studies in optics have considered dielectric crystals, where applications based on the phenomena mentioned above have

been proposed. In acoustics, contrarily, the interest has been focused mostly on the case of rigid scatterers [10], with a high impedance contrast with the surrounding medium, and less attention has been paid to the case of penetrable scatterers. However, the relevance of penetrable scatterers in acoustics is recovering a renewed interest, where applications as enhanced transmission through gratings [11] or the control of waves using arrays of penetrable cylinders in waveguides [12] have been recently proposed. Special interest appears for the case of low contrast systems [13].

Solid scatterers can be assumed to behave as rigid elements for acoustic waves when its reflectivity, which depends on the contrast of impedances of the scatterer and the host material, is high. On the contrary, if the impedance contrast is low (for example, the case of Al in water), a substantial part of the wave can propagate through the scatterer, which is considered as a penetrable element. In acoustics, this brings some additional complexities. Penetrability may break the analogy with the case of electromagnetic waves, since as the wave penetrates in the solid the sound-structure interaction becomes relevant, and transverse waves, corresponding to vibrations modes of the scatterers, can be easily excited, something like that has no analogue in electromagnetic wave systems. As a consequence, the assumption of longitudinal wave propagation becomes no more valid, and the dispersive characteristics of the system are altered [14].

Strictly speaking, dealing with only scalar sound waves under conditions of penetrability requires the use of fluid–fluid systems, i.e. fluid scatterers embedded in a fluid host. However, fluid–fluid composites present some drawbacks that makes them difficult to design, and are hardly realistic for experimental studies. There are still some proposals as composites made of mercury and water disposed in a boron nitride lattice, as presented in [9]. Another proposal consists of inserting a fluid inclusion into a latex bladder, but it is difficult to keep the structural integrity, and also some resonances can appear, arising from the elastic latex shell, that can perturb the properties of the system. And still a possibility is to implement such systems by porous scatterers with low absorption embedded in air, since porous materials can be treated as fluid-like materials over a wide range of frequencies [15]. However, the absorption due to the viscothermal losses, even being small, represents an inconvenient because they tend to drastically reduce the phenomena due to periodicity [16].

Here we show a physically realizable proposal to build a fluid-like, acoustically penetrable periodic system, overcoming some of the limitations of the above proposal. In the long wavelength regime, homogenization theories applied to periodic arrays of rigid inclusions embedded in a fluid medium allow to obtain the effective properties of the composite [17, 18]. In this regime, a cluster of rigid cylinders embedded in a fluid behaves like an equivalent fluid with effective mass density and sound velocity determined by the filling fraction of the cluster with small losses [19]. In this work, we propose a novel acoustic structure formed by a periodic distribution of such fluid-like scatterers in a fluid host medium. The resulting composite becomes a powerful alternative to develop fluid–fluid composites with high tunable properties of the medium within the penetrable scatterer. Structures based on a similar bottom–up approach, with an effective value of the permeability in the visible spectral domain, have been recently reported for optical waves [20, 21].

In the first part of this work, in section 2.1, we present the structure made of penetrable fluid-like structures and the analytical and numerical techniques used to study its behaviour. In section 2.2 we analyze both the scattering and the eigenvalue problems of a composite, and compare with the experimental results with a structure designed according the discussed theoretical assumptions. We find a good agreement that validates the main hypothesis. As an example of applicability of the proposed structure, in the remaining sections we present the acoustic analogues of two photonic phenomena: the focusing of unlocked evanescent waves [22] in section 3 and the coupled resonator waveguide [23] in section 4. Finally, the summary and conclusions of the work are discussed in section 5.

2. Acoustically penetrable sonic crystals

2.1. The penetrable structure

The proposed fluid-like structure consists of a periodic arrangement of clusters (large scale (mesoscopic) scatterers) made of a periodic distribution of N identical rigid scatterers, all embedded in a fluid. In the long wavelength regime ($\lambda >> a_s$, being λ the wavelength and a_s the distance between the rigid scatterers within the cluster) the cluster can be approximated as a fluid-like cylinder for acoustic waves with the following effective properties [19]

$$c_{\text{eff}} = \frac{c_0}{\sqrt{1+f_s}}, \tag{1}$$

$$\rho_{\text{eff}} = \rho_0 \frac{1+f_s}{1-f_s}, \tag{2}$$

where ρ_0 and c_0 are the density and sound velocity in the host material respectively and $f_s = S_s/S_c$ is the filling fraction of the cluster. S_s is the total area filled by the scatterers and S_c the area of the cluster. Therefore, by changing the filling fraction of the cluster, its mesoscopic physical properties such as the density and the wave velocity can be adjusted. The range of validity of such expressions are discussed in [19].

A possible scheme of a penetrable sonic crystal is shown in figure 1, where the scatterers are cylindrical clusters, each one formed by a small-scale periodic distribution of rigid square-rod scatterers. The system is embedded in a fluid. In this example, we have chosen the cylindrical clusters made of square rod scatterers, but it is worth noting that both the clusters and the scatterers can present different shapes. In this kind of structure the periodicities at both scales are characterized by two different lattice constants and two filling fractions. In the particular case shown in figure 1 we define the lattice constant, a, and filling fraction, $f = \pi R^2/a^2$, related to the arrangement of the cluster of radius R defining the sonic crystal, and the lattice constant, a_s, and the filling fraction $f_s = l_s^2 / a_s^2$ corresponding to the periodic structure of rigid square-rod scatterers with side length l_s. If the condition $a >> a_s$ is

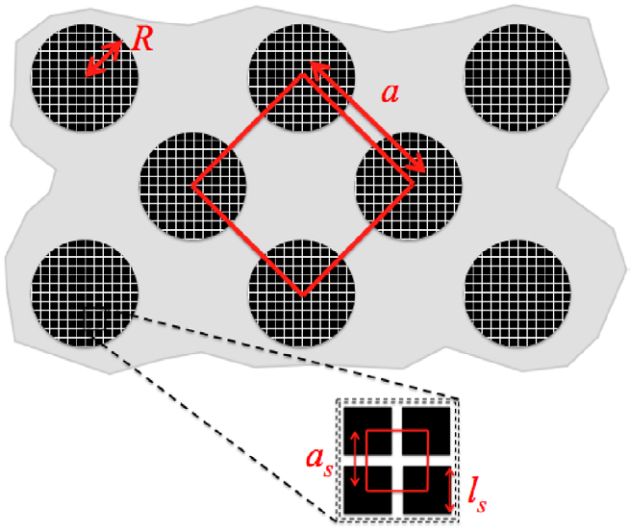

Figure 1. Scheme of the penetrable fluid–fluid system presented in this work. In this example we consider a two dimensional square array with lattice constant a and cylindrical inclusions of radius R. The inclusions are clusters of rigid square-rod scatterers with lattice constant a_s and length side l_s.

satisfied, the phenomena related to both scales of periodicity are uncoupled. Under this condition, for the range of frequencies in which $\lambda \simeq a$, the mesoscopic structure behaves like a fluid–fluid band gap material made of fluid-like clusters which properties can be easily tuned by changing f_s using equations (1) and (2). The main feature of the system is that it has double-periodicity, one in the long wavelength regime which determines the physical properties of the equivalent fluid of the clusters, and another one in the strongly dispersive regime that fixes the Bragg frequency and, more generally, the dispersion relation.

Through this work three different techniques have been used to evaluate the dispersion relations (eigenvalue problem) for different structures. We will solve both the ω (**k**) [24] and the $k(\omega)$ [25, 26] problems by means of different techniques based on plane wave expansion (PWE) [24–26] and finite element methods (FEM) [27]. In the case of periodic eigenvalue problem, the properties of the Bloch states constrain the solution to a unit cell with Bloch vectors in the first Brillouin zone. On the other hand, the scattering problem by an arrangement of penetrable cylinders is analyzed in this work using both the multiple scattering theory (MST) [2, 28] and the FEM. Either in the eigenvalue and the scattering problems, the continuity of both the pressure and velocity at the boundary of each scatterer is considered. Specifically for the case of the scattering problem, the T matrix for the multiple scattering of a penetrable fluid cylinder can be obtained considering the propagation of wave inside the scatterer [28].

2.2. Dispersion relation and scattering

Once the basic structure is introduced, in the following we show, numerically and experimentally, that the periodic arrangement of clusters behaves like a periodic fluid–fluid system. Notice that the concept of penetrable sonic crystal shown in this work is only restricted by the condition $a >> a_s$. Therefore independently of the mesoscopic lattice and the shape of the cluster or the inner periodicity, the concept is valid if the condition $a >> a_s$ is accomplished.

The structure presented in the previous section is too complex for an experimental design, since it contains a large number of elements. In order to make a simpler experimental arrangement, using a minimum number of elements, we consider a squared shape for the clusters (mesoscopic scatterers), while the small-scale elements (inner scatterers in the cluster) present cylindrical shape as shown in figure 2(*a*). Now the mesoscopic scatterer is a square cluster made of rigid, thin cylindrical rods with radius r_s, embedded in a air. Each cluster is an array of 4 × 4 rods, arranged in a square lattice with period $a_s = a/5$, being the filling fraction $f_s = \pi r_s^2 / a_s^2 = 0.4$. We notice that at this condition, the wavelength of the Bragg frequency for the mesoscopic scale, governed by a, is 5 times bigger than that of the small inner scale, governed by a_s. Therefore, considering the limits given in the [19], the cluster used here is in the long wavelength regime at normalized frequencies lower than 5/4. In this case, we study the behavior of the system up to the normalized frequency equal to 0.75. Then, the effective parameters of the cluster can be obtained from equations (1) and (2) and the effective properties are $c_{\text{eff}} = 0.8452\ c_0$ and $\rho_{\text{eff}} = 2.33\rho_0$. Using these parameters, we calculated the band structure of a square periodic distribution of these effective fluid square scatterers of length side $l = 3a_s + 2r_s$ with lattice constant a (see figure 2(*b*)), using the PWE method. We use this side length l because it defines the surface that interacts with the incident wave. Black continuous line in figure 2(*c*), represents the dispersion relation, i.e. the band structures calculated from the unit cell shown in figure 2(*b*). They are represented in normalized units with respect to both the lattice constant, a, and the properties of the host material presenting the band gap in the range [0.41, 0.5]. On the other hand, using FEM, we have calculated the band structure of the periodic distribution of the cluster of rigid scatterers, i.e. using the unit cell shown in figure 2(*a*). Red circles in figure 2(*c*) represent this band structure showing the band gap at [0.41, 0.5]. By comparison of these two results we conclude that the periodic distribution of clusters can be considered as a periodic fluid–fluid system. Moreover, in order to highlight the differences between fluid-like, and rigid-fluid composites, we also represent the band structures obtained for the cluster being acoustically rigid (red dashed lines) showing the different width of the band gap ([0.33, 0.56]) due to different contrast of impedance. Finally, for the sake of completeness we represent the band structure of the small scale periodic structure inside the cluster (blue dotted line), showing its linear part at low frequency regime and as a consequence the proof that validates its homogenization. To have a best comparison with respect to the band structure of the cluster, the Bloch vector has been normalized to a_s, so the x-axis for this band is shown in the upper horizontal axis (in blue), while the frequencies are normalized to the periodicity of the clusters, a.

The structure was designed experimentally. In particular, the cluster is made of aluminium cylinders of radius $r_s = 2$ cm

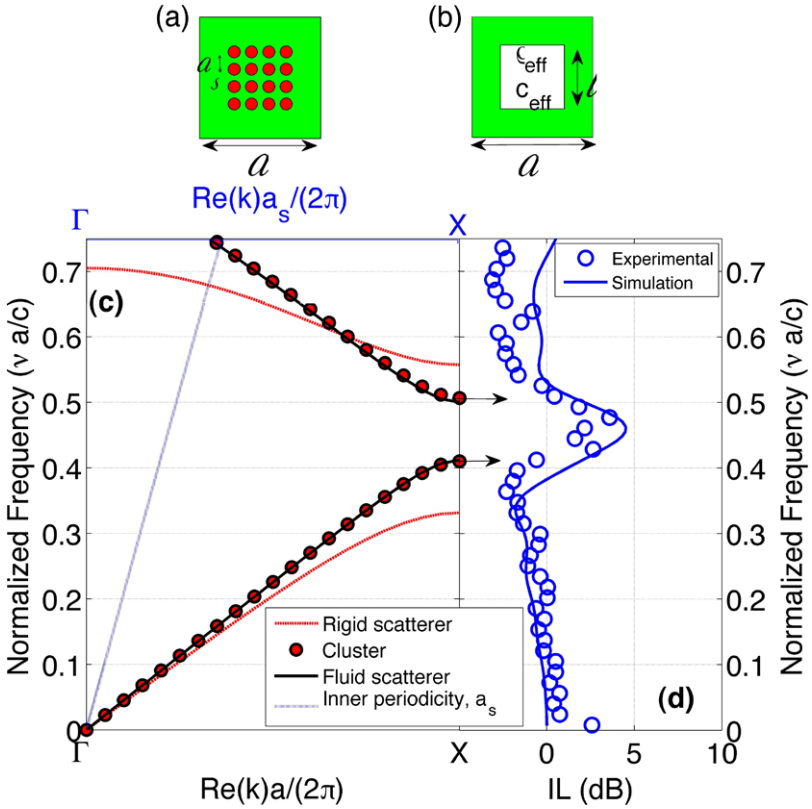

Figure 2. (*a*) Scheme of the unit cell of 2D square array of clusters. (*b*) Equivalent unit cell from the effective properties of the cluster shown in (*a*). (*c*) Band structures in the ΓX direction. The continuous black line (red dots) represents the band structure for the equivalent fluid–fluid structure (for the periodic arrays of clusters). Dashed red lines represent the band structures for the case in which the clusters are considered acoustically rigid. Blue dotted lines represent the band structure for the periodicity inside the cluster. We note that for this case the Bloch vector is normalized with respect to a_s, so the *x*-axis for this band is shown in the upper axis (in blue). (*d*) The continuous line represent the theoretical IL evaluated at $x = 3a$ of the fluid fluid composite, while open blue dots represent the experimental results.

embedded in air with an inner periodicity $a_s = 5.5$ cm. The periodicity of the square array of cluster is $a = 5a_s$. Details of the experimental set-up can be found in [6]. We have experimentally and theoretically (by means of MST) evaluated the Insertion Loss (IL) of the structure. The IL spectrum of an arrangement of scatterers is obtained measuring transmitted sound pressure levels, with and without the sample, at the same point. *IL* is determined as

$$IL = 20 \log_{10} \left| \frac{P_0(x)}{P(x)} \right|, \tag{3}$$

where $P_0(x)$ ($P(x)$) is the incident pressure (total pressure with the sample) calculated at x. In this work $x = 3a$ to avoid the edge diffraction effect.

Figure 2(*d*) shows the theoretical (continuous blue line) and experimental (blue dashed line with open circles) *IL* of a periodic array of 4 × 4 clusters with a unit cell as shown in figure 2(*a*). Note the agreement, in spite of the small number of elements used to build the structure. We observe an increase of the IL at frequencies [0.39, 0.52]. This attenuation band is narrower than that predicted for the rigid-fluid system (dashed red lines in figure 2(*c*)) but very close to the band gap predicted for the fluid–fluid composite (continuous line in figure 2(*c*)). This supports the hypothesis that the periodic distribution of clusters of scatterers actually behaves as a periodic fluid–fluid composite.

In what follows we report two acoustical phenomena which are expected to occur only in penetrable structures. Both have been discussed in the photonic case, however a realization in acoustic case requires of using fluid–fluid like structures as those proposed in this work.

3. Focusing of evanescent waves

It is commonly accepted that evanescent waves in band gaps lay at the edges of the Brillouin Zone (BZ), i.e. the period of the decaying field oscillations lock to the period of the crystal [5, 7]. Locking means that, as the frequency changes within the band gap, the real part of the wavevector remains fixed and takes the value at the edge of the BZ (only the phase of the mode is allowed to change). We recently showed [22] that, in photonics, besides the conventional locked evanescent waves, a new class of unlocked evanescent solutions exists in two-dimensional (2D) systems with low index contrast. The wave-vectors of these waves have a non zero imaginary part (responsible for the evanescent behaviour), but its real part (denoting its modulation) is not locked to the crystal but it also changes with the frequency within the gap. Additionally, the real part of wavevector shows a curved isofrequency contour, which has been related to different spatial effects on beam propagation [29–31]. Particularly, for the case of the unlocked

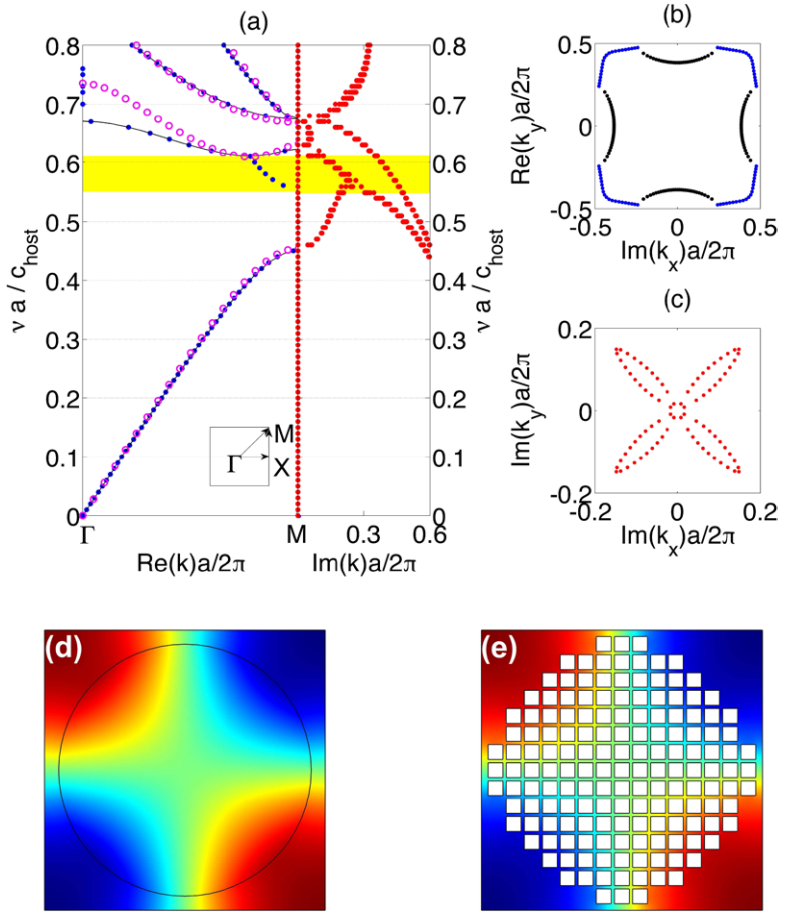

Figure 3. Dispersion relation of a square periodic fluid–fluid system ($\rho_{eff}/\rho_0 = 12.3$ and $c_{eff}/c_0 = 0.73$). The filling fraction is $f = \pi R^2/a^2 = 0.63$. The normalized frequency $\nu\ a/c_0$ and wave-vector $ka/2\pi$ are depicted. (*a*) Complex band structures. Blue dots in left panel show the real part and red dots in the right panel show the imaginary part obtained using the $k(\omega)$-methods (EPWE). For comparison, the continuous line in the left panel shows the band structures obtained using the $\omega(\mathbf{k})$-method (PWE). Purple open circles show the band structures of the systems calculated with the real cluster of rigid cylinders. (*b*) and (*c*) show real and imaginary parts of the complex isofrequency contours respectively for the normalized frequency $\nu\ a/c_0 = 0.58$. Black dots represents pure real eigenvectors, while blue and red dots represent the real and the imaginary parts of the complex wave-vectors respectively. (*d*) and (*e*) show the pressure field in the unit cell for the eigenvalue of the first band at point M [$(k_x, k_y) = (\pi, \pi)$] calculated with the equivalent fluid–fluid system and with the real cluster of rigid cylinders, respectively.

evanescent waves one expects that beams propagating at frequencies within the bandgap show focusing, in addition to evanescence. Therefore, these waves could be observed in a low contrast sonic crystal, and find its relevance in thin slabs of periodic materials. The goal of this section is to show the existence of unlocked evanescent waves in acoustics for penetrable periodic structures, and to show the focusing effect behind thin slabs produced by the unlocked real part of the wave vector. We will consider the analysis of a fluid–fluid structure, having in mind the structure proposed in the previous section.

3.1. Complex band structures

In a recent previous work, the problem of focalization of evanescent fields in a photonic crystal was discussed [22], and the parameters of the structure required to observe the phenomenon were estimated. Here we adapt the previous study to the acoustical case, and consider a square array of fluid cylinders of radius R with properties $\rho_{eff}/\rho_0 = 12.3$ and $c_{eff}/c_0 = 0.73$. Figure 3(*a*) shows the solution of the ω ($\mathbf{k}$) problem using PWE method for the system with a filling fraction $f = \pi(R/a)^2 = 0.63$ in the ΓM direction (see inset of figure 3(*a*)). This solution is shown with continuous black line, and it reveals a band gap in the range [0.45, 0.61] in normalized frequency units. Moreover, the complex band structures obtained from the problem $k(\omega)$, shown with blue and red dots, is a bit different. It is worth noting here that the overall number of bands at each frequency is preserved being the number of real bands equal to the number of imaginary ones. The complex band structures reproduce ($k(\omega)$ problem) the real-valued bands obtained from the ω ($\mathbf{k}$) but it yields the appearance of additional unlocked evanescent modes in the range of frequencies [0.55, 0.61] (shadowed area in figure 3(*a*)), where the real part of k is not constant, but depends on frequency. A careful inspection of figure 3(*a*) shows that at the lower part of the band gap the evanescent mode remains locked, while increasing the frequency the attenuation rates (imaginary part) of two

locked evanescent modes approach and merge, resulting in the appearance of an unlocked evanescent mode (shadowed area in figure 3(*a*)). This kind of evanescent modes connects the closest points of the dispersion curves from two adjacent propagation bands. However, if the frequency maxima and minima from both bands do not lay at high symmetry points of the Brillouin zone, as is the case for the locked evanescent waves, the modes become unlocked and cross the Brillouin zone as shown in figure 3(*a*).

Up to now, all the results have been discussed for the case of real fluid–fluid systems. Next, we use the periodic system of clusters to analyze its properties. For that, we consider a composite made of a cluster of cylinders with the following filling fractions: $f = 0.63$ and $f_s = 0.8$. The filling fraction f is the same as in the previous fluid–fluid system, shown in figure 3(*a*), and f_s reproduces the same sound velocity and density ratio as for the fluid–fluid system. Using the square rod scatterers, arranged in a square periodicity inside the cluster, we construct a quasi cylindrical inclusion (see figure 3(*e*) for the unit cell) with the desired physical properties. At this stage, we check that the periodic distribution of clusters reproduces the same properties as the fluid–fluid composite previously analyzed. Purple open dots in figure 3(*a*) show the band structures calculated from the ω (**k**) problem for the system made of clusters. Notice that the band structure calculated with the fluid–fluid composite and that corresponding with the periodic distribution of clusters are in good agreement. The discrepancies in the second band around the Γ point are due to two reasons. On one hand the non perfect cylindrical shape of the cluster and, on the other hand, that the filling fraction used for the cluster is near to the upper limit of validity of the equations (1) and (2). Figures 3(*d*) and (*e*) show the pressure field in the unit cell for the eigenvalue of the first band at point M [$(k_x, k_y) = (\pi, \pi)$] calculated with the fluid scatterer and with the cluster of rigid square-rod scatterers respectively. The agreement between the two eigen-fields is good.

In order to study the spatial effects of the non zero real part of the unlocked evanescent waves in the band gap, we have analyzed the complex isofrequency contours for the central frequency of the unlocked evanescent mode. As shown in [32], the spatially modulated materials, in addition to modify the temporal dispersion, are known also to modify the spatial dispersion (also called diffraction), allowing the managing of the diffractive broadening of the beams. Figures 3(*b*) and (*c*) show the real and the imaginary part of the complex isofrequency contours at the normalized frequency $\nu\ a/c_0 = 0.58$ respectively. Note that the real part of the isofrequency contour presents, along the ΓM (diagonal) direction, a region in which the curvature is positive. Positive curvatures in k-space (the convex case) introduce negative diffraction inside the periodic medium, which is afterwards compensated at some distance after the crystal by normal (positive) diffractive propagation in the surrounding fluid [29–31]. That distance is the focalization distance, so the system acts as a flat lens. Then, waves constructed from such unlocked evanescent modes can have a sufficient propagation freedom in order to develop curved wave-fronts. Then, we expenct that evanescent waves can be focused behind a thin flat–flat interface slice of periodic material.

3.2. Focusing of unlocked evanescent waves

The predicted focusing of evanescent beams is now demonstrated by direct numerical simulations using MST. The positive curvature of the real part of the isofrequency contours along the ΓM direction indicates that focusing of an evanescent beam behind a thin fluid–fluid system can be expected. To observe that, we consider a line source placed $5a$ from the crystal which end is placed at $x = 0$ and we evaluate the acoustic field behind several slabs with different number of rows.

Figures 4(*a*) and (*b*) show the acoustic pressure field, $|p|$, behind two slabs with 3 and 11 rows respectively. Notice that in both cases the end of the crystal corresponds to $x = 0$. One can clearly see both the focusing behaviour for the case of 3 rows and the decay of the amplitude of the focus as we increase the number of rows in the crystal, obviously because the effect is mediated by evanescent waves. Therefore the wider the crystal is, the smaller the amplitude of the focus is. During the process of calculation we have analyzed the acoustic profile shown in figures 4(*a*) and (*b*) for structures made of different number of columns, i.e. for more extended crystal in the y-direction. We have evidenced that the shape of the acoustic profile for a given number of rows does not change with the number of columns, so the effect of focusing by these structures is not an edge diffraction one but arising from the phase compensation outside the crystal creating the focus.

Figures 4(*c*) and (*d*) show the longitudinal and transversal cuts for different slabs with several number of rows. Due to the fact that the effect is due to evanescent waves, we can clearly see in the plots that an increasing of the number of rows implies a decreasing of the magnitude of the focus. As shown in [34] this decay is mediated by the imaginary part of the Bloch mode that characterized this evanescent mode. For the case of the 11 rows, we cannot talk about focusing because the evanescent mode is already attenuated through propagation in the crystal. However, even with 9 rows the magnitude of the focus is relevant and can have an effect behind the crystal.

4. Coupled resonator acoustical waveguide (CRAW)

The guiding of waves in periodic structures, making use of the presence of the band gap, is relevant in different applications in electromagnetism, optics and acoustics. As an example, a photonic crystal waveguide, formed by a line defect inside the crystal, can guide the light with high transmission efficiency in the sub-micron scale [7], which is very difficult to achieve for a dielectric waveguide. However due to the strong dependence of the band gap on the geometry of the system, the waveguiding using these mechanisms presents some disadvantages. A strong bend of the waveguide in the periodic structure implies large interior reflections and, as a

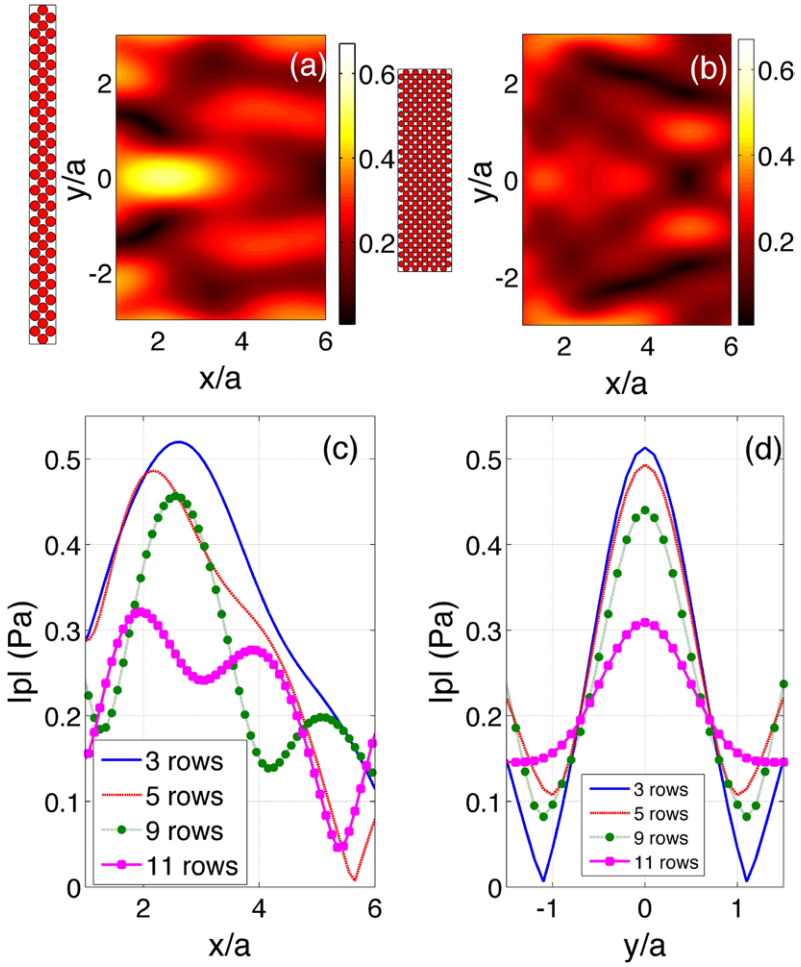

Figure 4. Transmission properties of several periodic slabs of the fluid–fluid system predicted by MST. (*a*) and (*b*) show the pressure field, $|p|$, for two slabs of 3 rows and 11 rows. (*c*) and (*d*) show the longitudinal and transversal cuts along the *x*-axis and *y*-axis, respectively, of (*a*) for different slabs with different numbers of rows.

consequence, a reduction of the efficiency of the waveguide. Moreover, the path of the waveguide must follow the specific lattice orientation of the periodic background and should be embedded in a wide enough periodic media to avoid the propagation loss, so the waveguide occupies much space in the transverse dimension [35, 36].

A different type of optical waveguide named coupled resonator optical waveguide (CROW) has been proposed [23]. A CROW consists of an array of coupled resonators with high quality factor (Q-factor), and the guiding of light is due to photon hopping [37] along the successive resonators. In this section, we study the transmission properties of an alternative kind of waveguides based on the distribution of penetrable acoustic scatterers that use index guiding mechanism [23]. The waveguide is formed by aligning a 1D array of penetrable scatterers in a fluid medium. This can be considered as an acoustic analogue of the CROW, so we call the system a coupled resonator acoustical waveguide (CRAW).

We analyze a 1D arrangement of fluid-like cylindrical clusters f radius $r = 0.4a$, where a is the distance between them in the array (lattice constant). The properties of the clusters are determined by the inner filling fraction, $f_s = 0.5$, therefore $c_{\text{eff}}/c_{\text{host}} = 0.82$ and $\rho_{\text{eff}}/\rho_{\text{host}} = 3.04$. These properties have been chosen to be in the limit of validity of equations (1) and (2). Whit that, the cluster present a resonance at the normalized frequency $\nu\ a/c = 0.78$, which corresponds to the first resonant mode of the penetrable scatterer shown in the inset of figure 5(*a*).

We excite the waveguide with the acoustic field shown in figure 5(*a*) at the normalized frequency $\nu\ a/c = 0.78$. The source is a piston-like with a radiating length of the order of the lattice constant of the array, a. Figure 5(*b*) shows the propagation of the acoustic field through the array of clusters. We can observe that the resonance is excited in all the clusters producing a propagation of the acoustic field through the array due to the coupling of the resonators in the array. In this system the coupling between resonators is strongly depending on the distance between the scatterers because the excited mode has a leakage to the free space. In figure 5(*c*) we show the profile along the the x-direction at $y/a = 0$. Blue line correspond to the case shown in the figure 5. We notice here that all the resonators are excited with almost the same amplitude along the array. Red and black lines show the cases of 1D arrays with the distance between scatterers equal to $4a$ and $8a$ respectively. We can observe that for these cases the resonant mode is excited in all the resonators but now the amplitude in

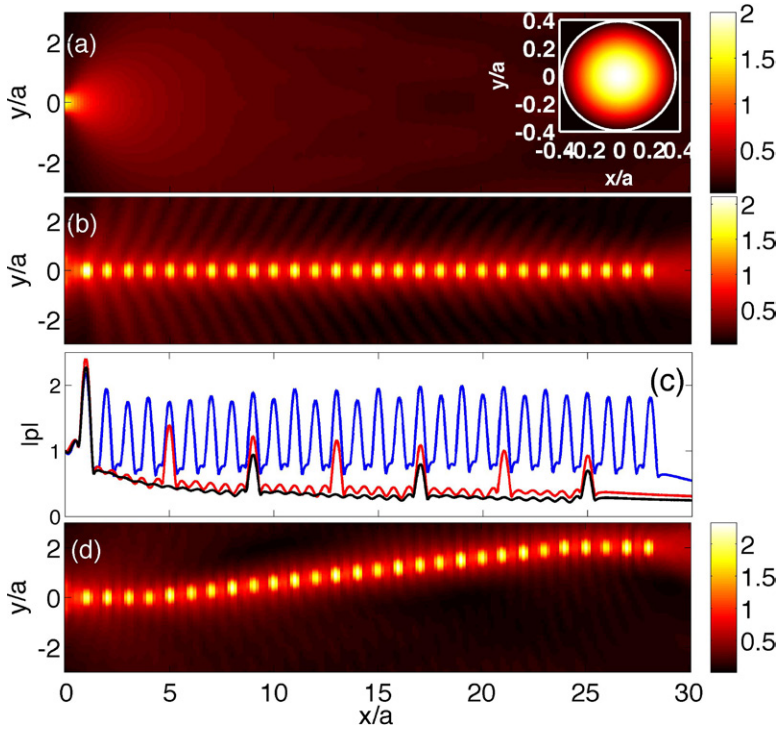

Figure 5. (*a*) Incident acoustic field at $\nu\, a/c_{\text{host}} = 0.78$. Inset shows the resonant mode of the fluid scatterer at $\nu\, a/c_{\text{host}} = 0.78$. (*b*) Guided waves at the resonant frequency, $\nu\, a/c_{\text{host}} = 0.78$, by a straight discrete distribution of 28 penetrable scatterers. (*c*) Longitudinal cuts of acoustic pressure, $|p|$, along the x-direction at $y/a = 0$ for the structure analyzed in (*b*) (blue continuous line), and for two 1D arrays where the lattice constants are $4a$ (red line) and $8a$ (black line), respectively. (*d*) Guided waves at the resonant frequency, $\nu\, a/c_{\text{host}} = 0.78$, by a bended discrete distribution of 28 penetrable scatterers. Color scale in maps show the values of $|p|$.

each resonator is reduced along the array, producing a small propagation of the acoustic field as the distance between scatterers is bigger.

To finish this section we show the possibility of guiding a wave through bended paths using a CRAW. Without loss of generality, we analyze a waveguide that has a input at $y/a = 0$ and the output is at $y/a = 2$ as shown in figure 5(*c*). Figure 5(*c*) shows the transmission through the waveguide by the activation of the index guiding mechanism for the first resonant frequency.

We can see in both cases that at the excitation frequency, the resonance of the penetrable scatterers is excited through the waveguide so the index guiding mechanism is activated and waves are transmitted through the waveguide. It is worth noting here that, as in the case of the optical counterpart (CROW), we assume sufficiently large separation between the individual resonators that the resonators has a weakly near field coupling. Consequently, we expect and we observe in figures 5(*b*) and (*d*) that the transmitted mode in such a coupled-resonator waveguide remains essentially the same as the mode in a single resonator (inset in figure 5(*a*)). At the same time, the far field coupling must be taken into account which is the responsible of the coupling in the array analyzed in this section. Such coupling is based on evanescent-field coupling, between the individual modes to explain the transmission of waves. Therefore, the coupling between the scatterers strongly depends on the distance between them as shown in figure 5(*c*). This coupling is an analogue of the tight-binding limit in condensed-matter physics, [33] in which the overlap of atomic wave functions is large enough that corrections to the picture of isolated atoms are required. The individual resonators in our waveguide are the analogue of the isolated atoms, and the resonant mode in the resonators corresponds to the atomic wave function.

5. Concluding remarks

We have proposed a periodic structure made of penetrable scatterers for scalar waves, the penetrable sonic crystals. The approach is based on the fluid-like behaviour of a cluster made of rigid scatterers. These clusters have their physical properties managed by the filling fraction of the micro-structure. Therefore, we propose here a double periodicity composite made of a periodic distribution of fluid-like clusters; one periodicity corresponds to large scale arrangement of the clusters, and the other periodicity corresponds to the small scale inside the cluster. Therefore the inner periodicity controls the physical properties of the fluid-like scatterer and the size and the distribution of the clusters the propagation properties of the penetrable sonic crystals. Analytical and numerical simulations show that the periodic distribution of clusters embedded in fluid is equivalent to the case of fluid–fluid periodic system with penetrable scatterers. Using this main property, we show here that the proposed structure can be used to observe the presence of unlocked evanescent waves and to design a coupled resonator waveguide for scalar waves. These fluid–fluid

systems could in practice pave the way to show several wave control phenomena in different branches of science and technology and extensions of this work can be developed to analyze periodic structures made of anisotropic scatterers.

Acknowledgments

We acknowledge financial support by Spanish Ministerio de Economia y Competitividad and European Union FEDER through project FIS2011-29731-C02-01 and -02. VRG is grateful for the financial support of the post-doctoral grant from the "Pays de la Loire". ACR is grateful for the support of the Programa de Ayudas e Iniciativas de Investigacin (PAID) of the UPV.

References

[1] Chew W C 1995 *Waves and Fields in Inhomogeneous Media* (New York: IEEE)
[2] Martin P 2006 *Multiple Scattering: Interaction of Time-Harmonic Waves with N Obstacles* (Cambridge: Cambridge University)
[3] Maurel A, Mercier J-F and Felix S 2014 *J. Acoust. Soc. Am.* **135** 165
[4] Martínez-Sala R, Sancho J, Sánchez J V, Gómez V, Llinares J and Meseguer F 1995 *Nature* **378** 241
[5] Brillouin L 1953 *Wave Propagation in Periodic Structures* 2nd edn (New York: Dover)
[6] Romero-García V, Sánchez-Pérez J V, Garcia-Raffi L M, Herrero J M, García-Nieto S and Blasco X 2009 *J. Acoust. Soc. Am.* **125** 3774–83
[7] Joannopoulos J, Johnson S, Winn J and Meade R 2008 *Photonic Crystals: Molding the Flow of Light* (Princeton, NJ: Princeton University)
[8] Sigalas M, Kushwaha M S, Economou E N, Kafesaki M, Psarobas I E and Steurer W 2005 *Z. Kristallogr.* **220** 765–809
[9] Pennec Y, Vasseur J O, Djafari-Rouhani B, Dobrzyski L and Deymier P A 2010 *Surf. Sci. Rep.* **65** 229–91
[10] Sánchez-Pérez J V, Caballero D, Martínez-Sala R, Rubio C, Sánchez-Dehesa J, Meseguer F, Llinares J and Gálvez F 1998 *Phys. Rev. Lett.* **80** 5325–8
[11] Maurel A, Mercier J-F and Felix S 2013 *Phys. Rev.* B **88** 115416
[12] Cai L W, Dacol D K, Calvo D C and Orris G J 2007 *J. Acoust. Soc. Am.* **122** 1340
[13] Maurel A and Mercier J-F 2012 *J. Acoust. Soc. Am.* **131** 1874
[14] Li F-L, Wang Y-S and Zhang C 2011 *Phys. Scr.* **84** 055402
[15] Allard J-F and Atalla N 2009 *Propagation of Sound in Porous Media: Modelling Sound Absorbing Materials* 2nd edn (London: Wiley)
[16] Umnova O, Attenborough K and Linton C M 2006 *J. Acoust. Soc. Am.* **119** 278
[17] Barryman J G 1980 *J. Acoust. Soc. Am.* **68** 1809
[18] Mei J, Liu Z, Wen W and Sheng P 2006 *Phys. Rev. Lett.* **96** 024301
[19] Torrent D and Sanchez-Dehesa J 2006 *Phys. Rev.* B **74** 224305
[20] Rockstuhl C, Lederer F, Etrich C, Pertsch T and Scharf T 2007 *Phys. Rev. Lett.* **99** 017401
[21] Yannopapas V and Vanakaras A G 2011 *Phys. Rev.* B **84** 085119
[22] Botey M, Cheng Y-C, Romero-García V, Picó R, Herrero R, Sánchez-Morcillo V and Staliunas K 2013 *Opt. Lett.* **38** 1890–2
[23] Yariv A, Xu Y, Lee R K and Scherer A 1999 *Opt. Lett.* **24** 711
[24] Kushwaha M, Halevi P, Martnez G, Dobrzynski L and Djafari-Rouhani B 1994 *Phys. Rev.* B **49** 2313
[25] Romero-García V, Sánchez-Pérez J and Garcia-Raffi L 2010 *J. Appl. Phys.* **108** 044907
[26] Laude V, Achaoui Y, Benchabane S and Khelif A 2009 *Phys. Rev.* B **80** 092301
[27] Ihlenburg F 1998 *Finite Element Analysis of Acoustic Scattering* (New York: Springer)
[28] Chen Y, Ye Z 2001 *Phys. Rev.* E **64** 036616
Chen Y and Ye Z 2001 *Phys. Rev. Lett.* **87** 1843011
[29] Notomi M 2000 *Phys. Rev.* B **62** 10696
[30] Kosaka H, Kawashima T, Tomita A, Notomi M, Tamamura T, Sato T and Kawakami S 1999 *Appl. Phys. Lett.* **74** 1212
[31] Pérez-Arjona I, Sánchez-Morcillo V J, Redondo J, Espinosa V and Staliunas K 2007 *Phys. Rev.* B **75** 014304
[32] Sánchez-Morcillo V J, Staliunas K, Espinosa V, Pérez-Arjona I, Redondo J and Soliveres E 2009 *Phys. Rev.* B **80** 134303
[33] Ashcroft N W and Mermin N D 1976 *Solid State Physics* (Philadelphia, PA: Saunders)
[34] Romero-García V, Sánchez Pérez J V, Castiñeira Ibáñez S and Garcia Raffi L M 2010 *Appl. Phys. Lett.* **96** 1241021
[35] Zhang M, Zhong W and Zhang X 2012 *J. Appl. Phys.* **111** 104314
[36] Escalante J M, Martínez A and Laude V 2014 *J. Phys. D: Appl. Phys.* **46** 475301
[37] Bayindir M, Temelkuran B and Ozbay E 2000 *Phys. Rev.* B **61** R11855–8